CT-Guided Stereotaxis Using a Modified Conventional Stereotaxic Frame

Philip J. Dubois[1]
Blaine S. Nashold[2]
John Perry[3]
Peter Burger[4]
Kevin Bowyer[5]
E. Ralph Heinz[1]
Burton P. Drayer[1]
Sandra Bigner[4]
Alfred C. Higgins[2]

Computed tomographic (CT)–guided stereotaxic procedures have become established in a few major centers but a single optimal system has not yet emerged. At Duke University Medical Center, availability of a stereotaxic frame with design features that lend themselves to CT adaptation made modification of this unit, rather than construction of a new dedicated frame, cost-effective. As other centers may seek to modify available stereotaxic equipment in a similar way, this report documents the modifications and the early clinical experience in four patients in whom CT-guided stereotaxic biopsy procedures were performed.

Computed tomographic (CT)–guided stereotaxis is now an established technique with proven clinical efficacy and safety [1–5]. Although at least three clinically proven CT stereotaxic frames are potentially available for purchase, the inevitable delay in their availability due to regulatory requirements and precision manufacturing, as well as their relatively high cost, make modification of existing conventional stereotaxic frames for CT techniques a worthwhile consideration. At our institution, a large number of conventional stereotaxic procedures are performed each year using the Todd-Wells stereotaxic system. A second stereotaxic frame, the Reichert-Mundinger system, receives relatively little use and was therefore available for adaptation to CT-guided stereotaxis. The modified system has proven clinically useful in four patients to date, with an accuracy of probe placement to within 1 mm in cadaver and phantom experiments. Because other institutions may find adaptation of available instrumentation preferable to purchase or construction of a dedicated CT stereotaxic frame, a description of these modifications and early clinical experience may be useful.

Unmodified Reichert-Mundinger Frame (fig. 1)

A base ring is attached by four removable clamps and threaded tapered pins to the calvaria. A removable "bow" is attached to the base ring by two removable fulcrum pins at the 90° and 270° positions on the base ring. Also attached to the base ring is a curved calibrated supporting bar that can be mounted anteriorly (0°) or posteriorly (180°). The "bow" is offset so that instruments held in the zero position by an electrode carrier are in a plane passing through the fulcrum of the "bow" as the latter is rotated. The electrode carrier has calibrated angular adjustments, which permit movement of instruments (probes, stimulating or recording electrodes, or biopsy needles) in the "x" (coronal) and "y" (sagittal) axes. A linear scale determines the depth ("z" axis) to which an instrument is introduced. Additionally, the electrode carrier may be moved along the "bow" from side to side permitting lateral, vertical, or intermediate approaches to the calvaria. Removable stainless steel pins (not shown) are attached at precisely determined locations along the base ring perpendicular to its upper surface as reference points for frame alignment and mensuration by radiographs made

Received July 15, 1981; accepted after revision November 10, 1981.

[1] Division of Neuroradiology, Department of Radiology, Box 3808, Duke University Medical Center, Durham, NC 27710. Address reprint requests to P. J. Dubois.

[2] Division of Neurosurgery, Duke University Medical Center, Durham, NC 27710.

[3] Pfizer Medical Systems, Columbia, MD 21045.

[4] Division of Neuropathology, Duke University Medical Center, Durham, NC 27710.

[5] Division of Computer Science, Duke University Medical Center, Durham, NC 27710.

AJNR 3:345–351, May/June 1982
0195-6108/82/0303-0345 $00.00

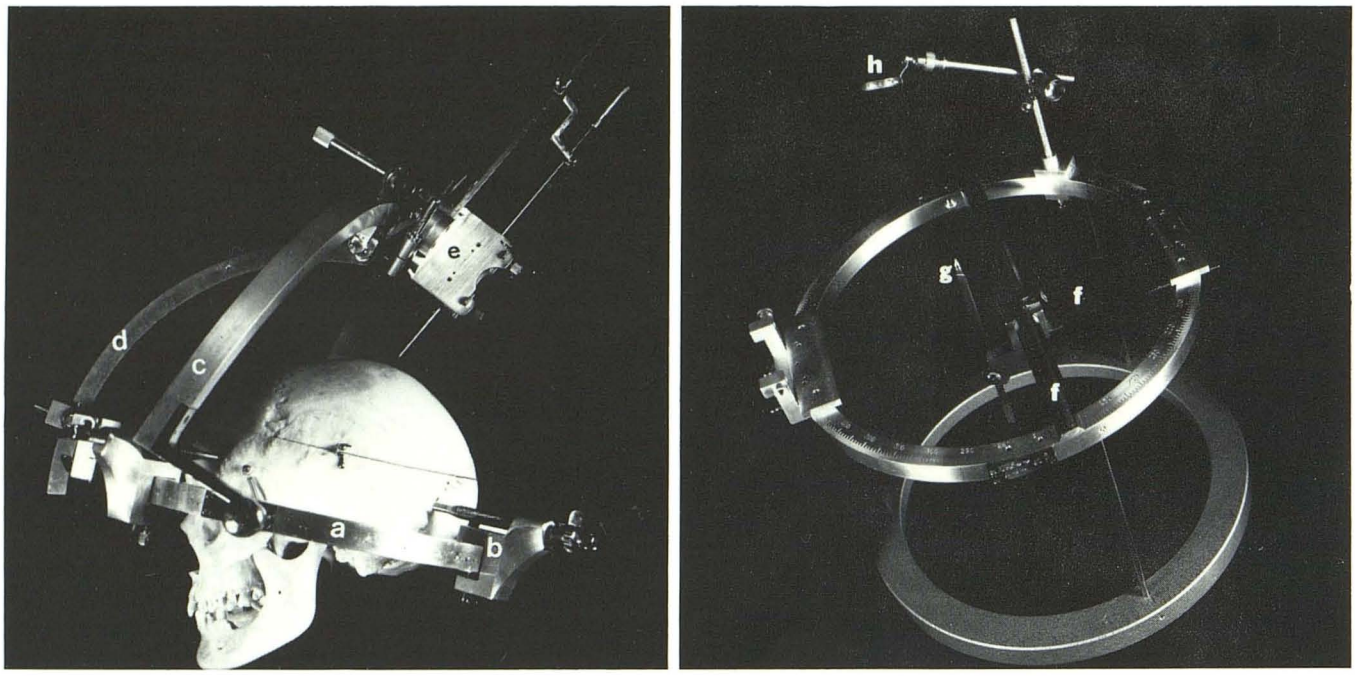

A B

Fig. 1.—**A**, Original Reichert-Mundinger frame: (a) base ring; (b) head fixation clamp; (c) "bow"; (d) supporting bar; (e) electrode carrier. **B**, Phantom ring is exact replica of base ring except for attached linear scale system (f) with target (g). Intracranial target zones are duplicated by target, operative approach is planned, and "bow" is transferred with support bar and electrode carrier back to patient base ring. Removable localizing ring for burr hole position (h).

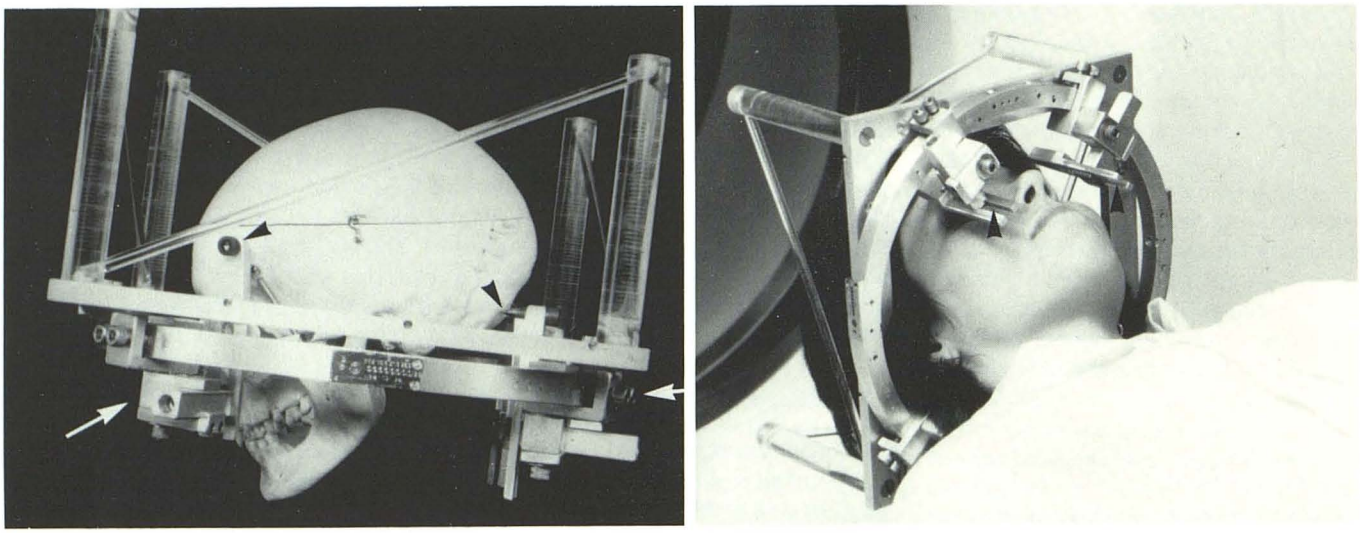

A B

Fig. 2.—Modifications for CT stereotaxis. **A**, Lucite fiducial rod system with aluminum supporting base attached to base ring which in turn is attached by adjustable clamps (*arrows*) and aluminum bars with steel pins (*arrowheads*) to calvaria. **B**, Aluminum bars of head fixation apparatus slotted (*arrowhead*) to adjust height of base ring and can be rotated to conform to skull contours or moved centrifugally for larger skulls.

during the conventional stereotaxic operation.

A "phantom" ring (fig. 1B) is an exact replica of the base ring with attached linear metal scales enabling the operator to position a metal target to correspond to an intracranial target when its linear frame coordinates in the "x" (coronal), "y" (sagittal), and "z" (depth) axes are known. Conventionally, these intracranial targets and their coordinates are derived from the intraoperative stereotaxic radiographs and

standard reference atlases [6].

The "bow" is attached to the phantom ring and a suitable angle of approach to the target determined. If an existing burr hole is to be used, its position in space can be defined on the phantom ring by initially attaching the "bow" to the base ring that is mounted on the calvaria, recording the angular and depth coordinates of the tip of a probe at the center of the burr hole, and mimicking this position with a second metal target attached to the phantom ring (fig. 1B). Once the surgical approach is determined at the phantom ring, the support bar position, angulation and depth of instrument, and electrode carrier position are then known and the "bow" is attached to the base ring for completion of the procedure. Accuracy of the predicted instrument path can be checked with conventional radiographs.

Modification for CT Stereotaxis

Localizing or "Fiducial" Rods

The principles for calculation of the x, y, and z coordinates of a target using three sets of lucite rods attached in a known relationship to the stereotaxic frame have been described by Brown [7]. In each rod set, two rods are perpendicular to the base ring and one is slanted. In the present

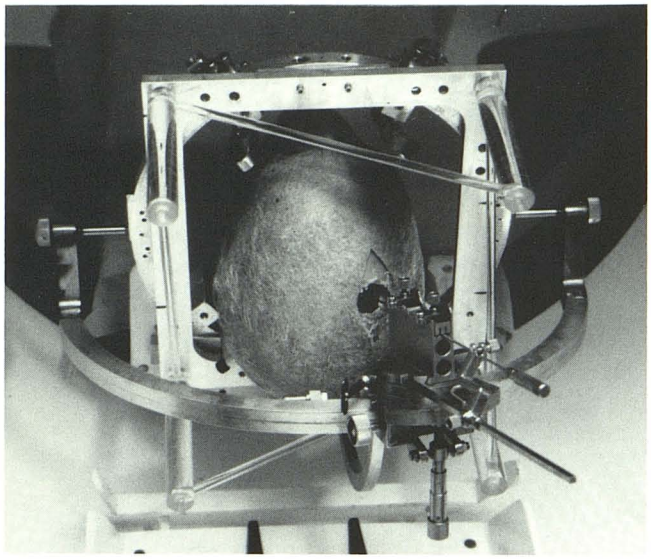

A

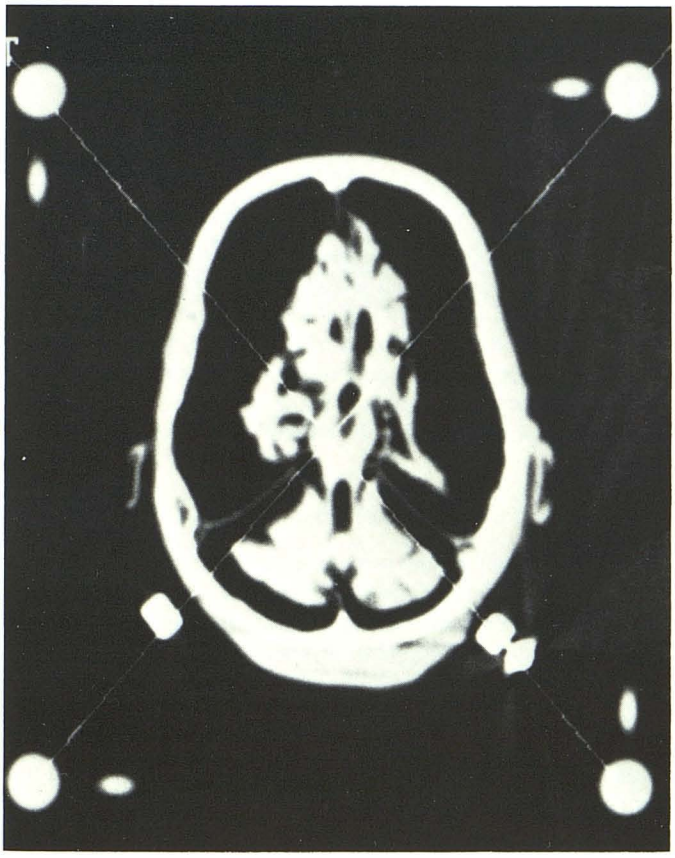

B

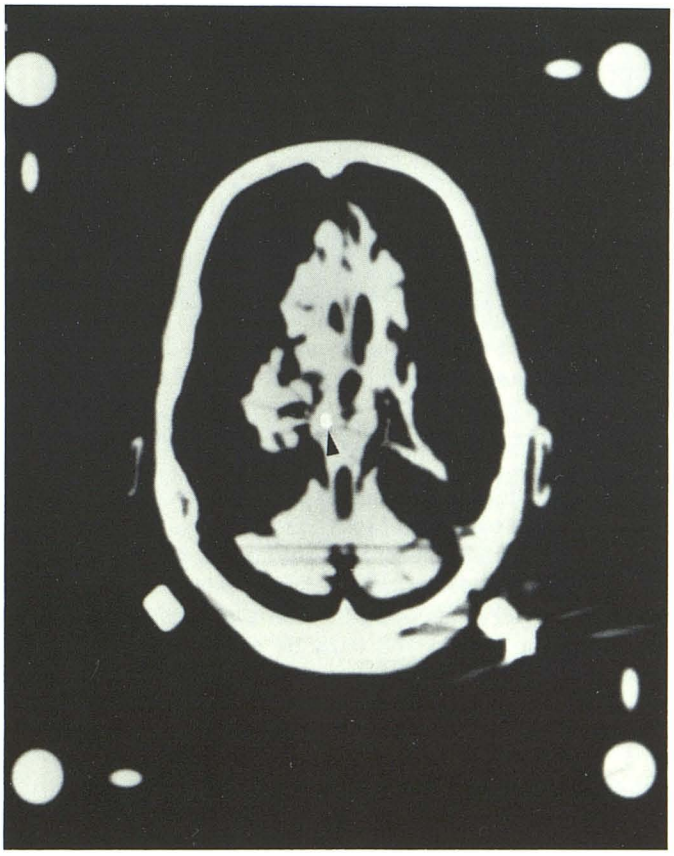

C

Fig. 3.—Cadaver biopsy experiment. **A**, Cadaver head in position with "bow" attached and probe inserted after calculation of target position and approach on phantom frame. **B**, CT image before placement of "bow" and probe. Target was defined in mesencephalon (intersection of lines). **C**, After computed calculation of target coordinates, probe (retouched) (*arrowhead*) corresponds exactly to designated target. Artifacts are generated by metal probe tip, and by aluminum "bow," the latter over cerebellum.

work, four such rod sets were attached to the base ring (fig. 2) centered at 0°, 90°, 180°, and 270° so that the three rod sets that lay closest to the designated target points in a clinical situation could be selected for greatest accuracy [3]. Initially, we used relatively small sets of rods attached to the base ring to permit a full range of rotation of the "bow," but in phantom experiments, errors as great as 4 mm were encountered in final probe tip positions. This rod system was therefore abandoned in favor of the system illustrated in figure 2 in which the larger diameter perpendicular rod heights are 12 cm and the distances between these rods measure 21.5 cm (y, or sagittal axis) and 24 cm (x, or coronal axis) (Prototype system, Pfizer, Columbia, MD 21045). The large perpendicular rods have a diameter of 18 mm; the slanted rods, 6 mm. The rod system is mounted on a flat aluminum plate which in turn is fixed to the base ring by set screws and two adjustable shims of 3 mm thickness at the 0° and 360° positions. The shims serve two purposes. First, they allow free space for attachment of the head-holding clamps, and second, they permit precise adjustment so that the center of the rectangle formed by the vertical rods corresponds exactly to the center of the base ring. Although the large rod system limits excursions of the "bow" anteriorly and posteriorly, it permits much greater accuracy, never exceeding 1 mm in experimental probe placement in phantoms and cadavers.

Computer Program for Fiducial Transformation

Calculation of the linear phantom frame coordinates (x, y, z) from a CT image of a designated target requires a transformation of the CT coordinates (x, y, z) to frame coordinates (x^1, y^1, z^1). Software modification to the Pfizer 0450 CT scanner [3] enables the operator to input the fiducial rod positions and the desired target positions using a track-ball cursor at the CT scanner console and simple interactive procedures at the console keyboard yield the frame coordinates in less than 2 min of operator time. A further software modification involved creation of a new 30 cm diameter field of reconstruction so that the fiducial rod system could be encompassed in the image.

A similar computer program for transformation of CT to frame coordinates has been developed on a handheld programmable calculator (Hewlett Packard HP41CV, Andover, MA 01810) so that CT stereotaxic procedures can be performed on the different scanners available at our institution. The procedure is less streamlined and potentially less accurate, however, since the CT x and y coordinates of the center of each fiducial rod must be estimated by manual cursor positioning and entered by hand into the calculator. This procedure takes about 5 min of operator time.

Modification of Head Clamps

The original head fixation devices were inappropriate and were replaced by adjustable thin aluminum bars similar in principle to those used in the Karolinska system [8] (fig. 2).

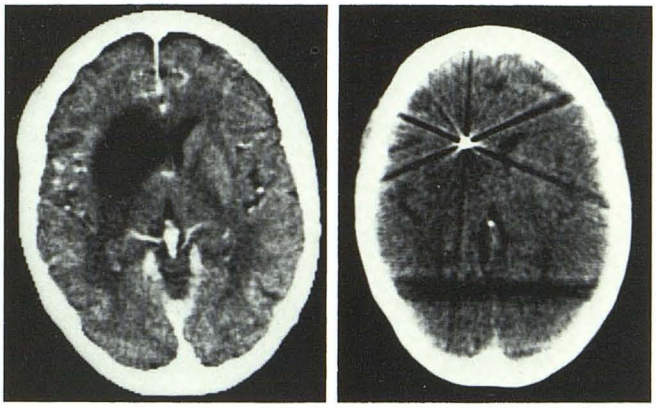

A B

Fig. 4.—Cerebral mucormycosis. **A**, Low density lesion with minimal mass effect in basal ganglia effacing right frontal horn. **B**, Placement of biopsy probe within lesion using CT calculation of stereotaxic coordinates. Artifact from aluminum "bow" overlies occipital lobes.

The modified clamps permit the use of aluminum bars of different lengths and curvature to parallel the calvarial contour so that the base ring can be applied low enough to avoid artifacts from the baseplate appearing in the scan plane containing the target area. Similarly, high or low positions of threaded holes in the bars allow the steel pins that screw into the calvaria to be placed appropriately to avoid artifacts in the plane of the target lesion. Artifact generation from the relatively thin aluminum bars has not been significant in clinical practice.

Mounting the Frame to the Pallet

A modified curved cushioned pallet has permanently attached two vertical steel bars to which the baseplate is attached by two quick-release clamps. To provide maximum ease of access to the calvaria and head frame, the patient lies on this modified pallet, which is fixed by locating pins to the "back bed" of the scanner. In case of anesthetic or surgical emergency, quick-release clamps enable the patient to be removed from the scanner in a matter of seconds.

Phantom and Cadaver Experiments

Initially, small metal targets were suspended in space within the fiducial rod system, and when CT was performed to frame coordinate transformation of the imaged metal target, it was found that a probe could be reliably introduced after modeling on the phantom ring and target assembly to within 1 mm of the metal target.

Figure 3 shows a cadaver experiment in which a probe was introduced into an arbitrary point designated within the brainstem together with the final probe position. Six such experiments were carried out and in each case the final probe position was within 1 picture element (1.0 mm) of the designated target in the x and y axes; using 2 mm slice

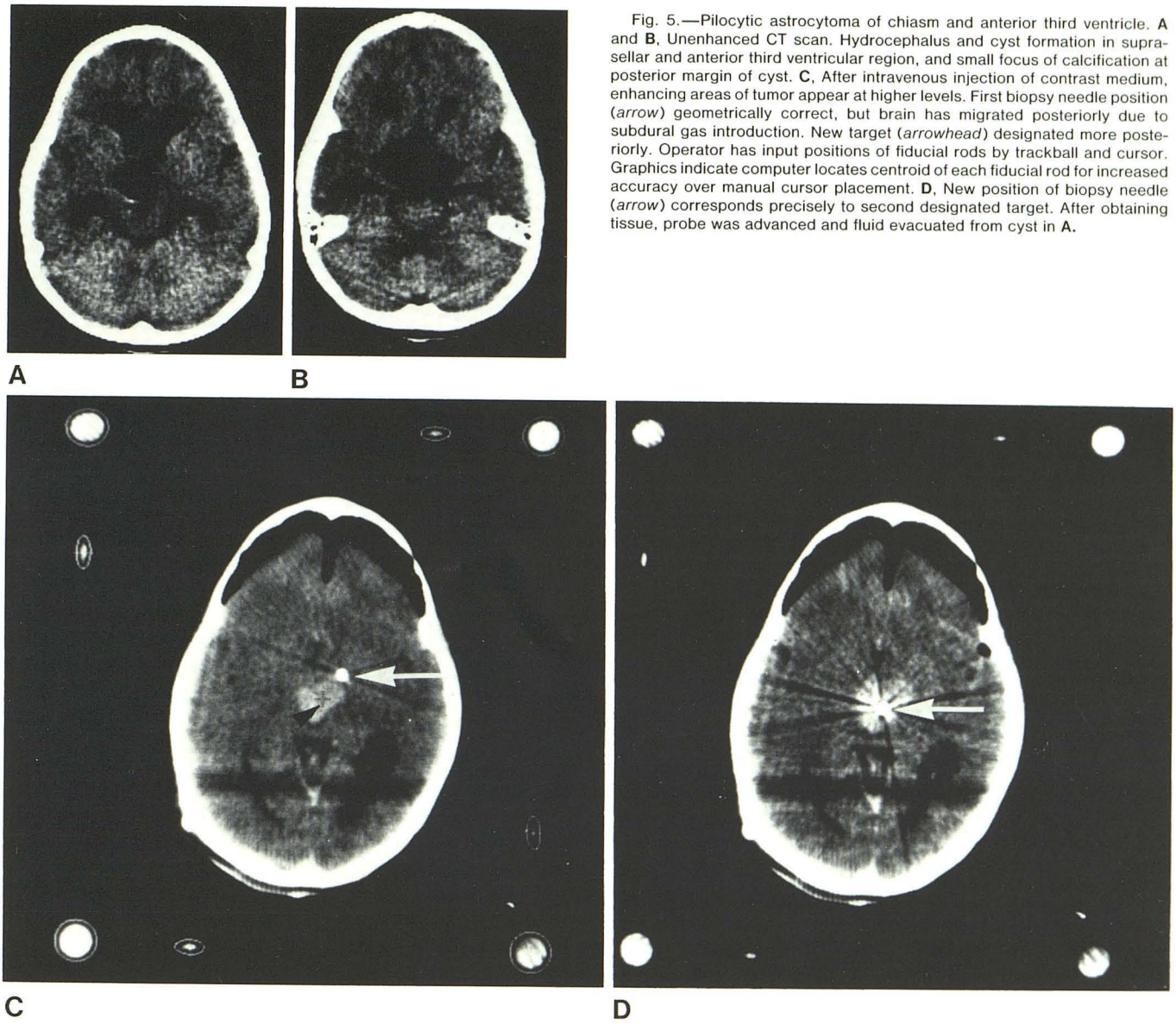

Fig. 5.—Pilocytic astrocytoma of chiasm and anterior third ventricle. **A** and **B**, Unenhanced CT scan. Hydrocephalus and cyst formation in suprasellar and anterior third ventricular region, and small focus of calcification at posterior margin of cyst. **C**, After intravenous injection of contrast medium, enhancing areas of tumor appear at higher levels. First biopsy needle position (*arrow*) geometrically correct, but brain has migrated posteriorly due to subdural gas introduction. New target (*arrowhead*) designated more posteriorly. Operator has input positions of fiducial rods by trackball and cursor. Graphics indicate computer locates centroid of each fiducial rod for increased accuracy over manual cursor placement. **D**, New position of biopsy needle (*arrow*) corresponds precisely to second designated target. After obtaining tissue, probe was advanced and fluid evacuated from cyst in **A**.

thickness, the z axis position was estimated to be within 2 mm in all experiments.

Case Reports

Case 1

A 59-year-old woman receiving high dosage steroids for plasma cell pneumonitis was admitted complaining of left upper and lower limb weakness of 12 hr duration. A mild left hemiparesis progressed to dense flaccid hemiplegia over 2 hr and there was rapid decline in mental status. Emergency CT revealed a low-density, nonenhancing, well circumscribed lesion in the right basal ganglia with minimal mass effect (fig. 4A). These CT and clinical features were atypical for abscess, infarction, or tumor, and emergency frontal lobectomy and biopsy of the lesion were contemplated as life-saving measures and to obtain a tissue diagnosis. As a less invasive alternative, a 14-gauge biopsy needle was introduced using CT-guided stereotaxis without the need for general anesthesia (fig. 4B). The tissue obtained consisted of necrotic brain. Large irregular nonseptated hyphae infiltrated the walls of the blood vessels and extended focally into the surrounding parenchyma. Fungal cultures of the biopsy specimen recovered *Mucor*. Amphothericin B therapy was begun, but the lesion continued to enlarge at two successive CT examinations and the patient died 4 days after admission.

Case 2

A 6-year-old girl presented with a long history of poor bilateral visual acuity and recent headache and vomiting. She also showed signs of growth retardation. CT (fig. 5) demonstrated marked hydrocephalus with a partly calcified, partly cystic, inhomogeneously-enhancing suprasellar mass. CT-guided biopsy was attempted to differentiate between craniopharyngioma and cystic chiasmatic/

hypothalamic glioma. At first passage of the biopsy needle, an attempt was made to sample enhancing solid tissue. Although the probe position corresponded exactly to the designated target, normal brain tissue was obtained. Probe introduction was accompanied by entry of subdural gas (fig. 5C) so that the target had, in effect, moved posteriorly. A new target was designated and with a second biopsy needle (fig. 5D), diagnostic tissue was obtained. The needle was then advanced into the cystic component and about 10 ml of yellowish fluid was obtained. This fluid was much more typical of glioma than craniopharyngioma, but confident differentiation between reactive gliosis and astrocytoma could not be made histologically. Accordingly, an open biopsy was performed and the diagnosis of a pilocytic astrocytoma was established histologically. Radiation treatment was begun.

Case 3

A 16-year-old boy presented with a focal right arm seizure followed by a grand mal seizure. There was a history of longstanding rheumatic valvular heart disease, and he had had a recent febrile illness. Neurologic examination demonstrated a mild right hemiparesis. CT examination revealed an enhancing ring lesion deep in the left parietal lobe extending to the left thalamus with marked mass effect and surrounding edema (fig. 6A). The most likely diagnosis was an intracerebral abscess secondary to bacterial endocarditis. Using CT-guided stereotaxis, a flexible catheter was introduced to the center of the ring lesion (fig. 6B) for aspiration, drainage, and antibiotic instillation. The fluid was yellow, and though thicker than cerebrospinal fluid, was not purulent. Therefore, a 14-gauge, blunt-tipped biopsy probe was introduced along the same approach after removal of the drain. Tissue obtained from the wall of the ring lesion was diagnostic of a pilocytic astrocytoma (figs. 6C and 6D). Radiotherapy and chemotherapy were instituted.

Case 4

A 44-year-old man presented with a 2 year history of weakness and clumsiness in the right arm, intermittent difficulty in expressing himself, and a recent generalized seizure after involuntary jerking movements of the right arm. Neurologic examination showed a right hemiparesis with hyperreflexia (maximal in the upper extremity), mild dysnomia, and decreased sensation to pin prick in the right face. CT revealed multiple small enhancing nodules within the deep white matter of the left cerebral hemisphere and in the left basal ganglia. There was minimal mass effect and no evidence of surrounding edema. Review of a CT scan performed at another institution 1 year earlier showed that the same lesions were present but less well defined. Differential diagnosis included atypical metastases, demyelinating disease, multifocal glioma, and primary lymphoma of the brain. The most accessible lesion to biopsy, in the left posterior frontal lobe white matter, was about 7 mm in diameter, and CT-guided stereotaxis yielded pathologic tissue on three successive passes of the biopsy needle. Interpretation of the pathologic material was difficult as it contained abnormal numbers of astrocytes and prominent perivascular lymphocytes. An open surgical biopsy of the same lesion was performed after CT confirmed residual pathologic enhancement at the biopsy site. The surgeon encountered considerable difficulty locating the small pathologic area within the centrum semiovale. The pathologic tissue did not yield further helpful information in the interpretation of histology. Although the histologic findings were not diagnostic, the clinical and radiologic findings were considered most compatible with primary lymphoma of the brain, and radiation treatment was begun.

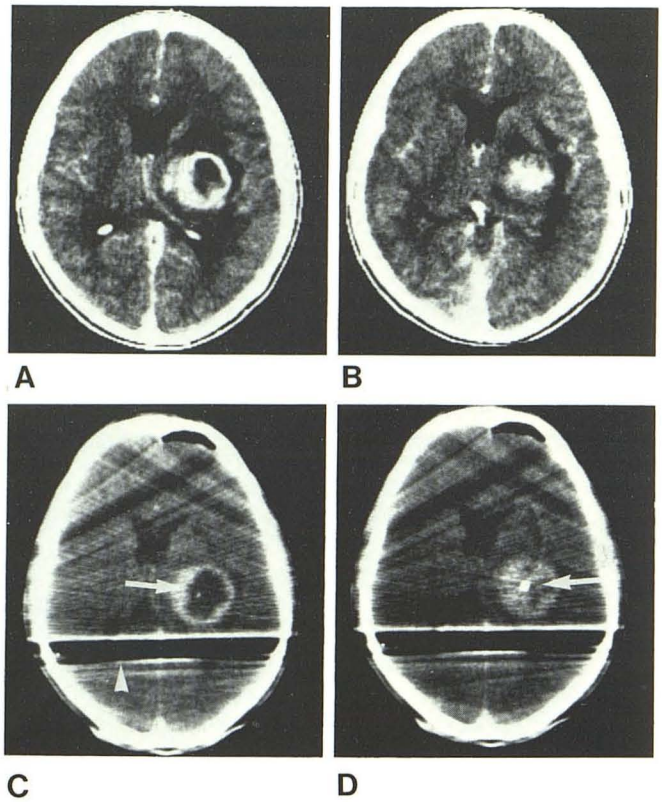

Fig. 6.—Pilocytic astrocytoma, left thalamic-deep temporoparietal region. **A** and **B**, Prominent irregular marginal enhancement, mass effect, and surrounding edema together with history of rheumatic heart disease and patient's age suggested abscess as more likely diagnosis than tumor. **C**, CT scan after placement of red rubber drain (*arrow*) over stereotaxic probe. Artifact (*arrowhead*) from "bow" still in position while fluid was aspirated. **D**, Introduction of biopsy probe (*arrow*) imaged at slightly lower level from which diagnostic tissue was obtained.

Discussion

Although the chief advantage in modifying an existing stereotaxic frame for CT-guided techniques is the reduced expense, numerous other advantages of this system have become apparent in clinical use. First of these is the immediate availability of a system when commercially available stereotaxic frames have yet to be approved for marketing. Next is the wide range of available instrumentation designed for use with the Reichert-Mundinger frame. These include sophisticated biopsy needles, stimulating and recording electrodes, a specially designed "endoscope" [9], and a twist drill that is fitted to the guide rails of the electrode carrier, which we anticipate will considerably decrease the time of the operation. At present an appropriate burr hole is made in the operating room, and the frame is fitted to the head in the CT scanning suite.

Several other advantages of the system emerged from the experience with these four patients. In case 1, the CT-guided technique provided a tissue diagnosis rapidly and effectively without the need for anesthesia. When clinical deterioration was paralleled by CT-demonstrated extension

of the lesion, unwarranted continuation of life support systems could be obviated.

The advantage of a CT stereotaxic system (with the capability for imaging the probe position), over a system where coordinates are calculated and the patient transferred to the operating room for "blind" biopsy, is well illustrated by the second patient in whom subdural gas caused shift of the target. Similarly, conducting the biopsy procedure within the CT suite in case 3 enabled the alteration of a planned drainage procedure to a definitive biopsy of a designated portion of the wall of the lesion.

In case 4, the ability to reliably introduce a biopsy needle to within 1 mm of a designated target made the CT-guided stereotaxic procedure less difficult than open biopsy because of the small size of the lesion. The difficulty in characterizing this particular lesion histologically both in this case and in case 2 reflected the histologic composition of the lesions rather than any technical shortcomings of the biopsy procedure. It is not unreasonable to assume that as more experience is gathered, a more confident histologic diagnosis may be made from the CT-guide biopsy specimens, thus precluding further surgical intervention in such cases.

Inevitably, there are limitations in any system that is modifed for purposes beyond those for which it was originally designed. The artifacts generated by the aluminum "bow" are only problematic when a target lies within the area of artifact. Horizontal biopsy needle approaches are not possible unless one or more of the rod sets are removed, thus limiting the flexibility of the system for selecting new targets after initial biopsy. Finally, as with other systems, the diameter of the localizing rod system places a lower limit on the field of reconstruction so that it is impractical to have smaller pixel sizes to create high resolution images of the thalamus, the amygdala, the commissures, and mesencephalon needed for functional stereotaxis. Alternatives to the use of extracranial localizing rod systems, to enable smaller fields of reconstruction and high spatial resolution magnified images of these structures [10], are currently under investigation.

ACKNOWLEDGMENT

We thank the neurosurgeons and neurologists of Duke University Medical Center for referring these patients for biopsy procedures; Myra Clark and Robin Sharpe for assistance with the procedures; the technologists of the Neuroradiology Division for performing the CT studies; and Rose Boyd for typing the manuscript.

REFERENCES

1. Lewander R, Bergstrom M, Boethius J, et al. Stereotactic computer tomography for biopsy of gliomas. *Acta Radiol [Diagn]* (Stockh) **1978**;19:867–888
2. Brown RA, Roberts T, Osborn AG. Simplified CT-guided stereotaxic biopsy. *AJNR* **1981**;2:181–184
3. Perry JH, Rosenbaum AE, Lunsford LD, Swink CA, Zorub DS. Computed tomography guided stereotactic surgery: conception and development of a new stereotactic methodology. *Neurosurgery* **1980**;7:376–381
4. Boethius J, Bergstrom M, Greitz T. Stereotaxic computerized tomography with a GE 8800 scanner. *J Neurosurg* **1980**;52:794–800
5. Huk W, Baer V. A new targeting device for stereotaxic procedures within the CT scanner. *Neuroradiology* **1980**;19:13–17
6. Schaltenbrand G, Wahren W. *Atlas for stereotaxy of the human brain, 2d* ed. Chicago: Year Book Medical, **1978**
7. Brown RA. A stereotactic head frame for use with CT body scanners. *Invest Radiol* **1979**;14:300–304
8. Greitz T, Bergstrom M, Boethius J, Kingsley D, Ribbe T. Head fixation system for integration of radiodiagnostic and therapeutic procedures. *Neuroradiology* **1980**;19:1–6
9. Shelden CH, McCann G, Jacques S, et al. Development of a computerized microstereotaxic method for localization and removal of minute CNS lesions under direct 3-D vision. *J Neurosurg* **1980**;52:21–27
10. Kozlow M, Abele MG, Griffith RC, Mair GA, Chase NE. Stereotactic surgical system controlled by computed tomography. *Neurosurgery* **1981**;8:72–82